

Experimental Validation of Energy Harvesting-System Availability Improvement Through Battery Heating

Daniel Cesarini, Vana Jelcic, *Student Member, IEEE*, Marijan Kuri, Mauro Marinoni, Davide Brunelli, *Senior Member, IEEE*, and Vedran Bilas, *Senior Member, IEEE*

Abstract—Operation of wireless sensor nodes or battery powered embedded systems in cold and harsh environments requires careful battery selection and management. In this paper, we first provide a general model of an energy harvesting sensor system and the respective energy flows. We then present a maximum power point tracking solar harvesting system according to that model. The system is coupled with rechargeable Li-ion batteries and equipped with a battery heating mechanism. The significant signals of that system are monitored to have a deeper insight into the energy distribution. Real-world experiments demonstrate benefits of battery heating during high irradiation periods at temperatures below safe charging conditions. The presented case study for a cold winter day shows that the additional energy, which can be stored thanks to battery heating would more than double the autonomy of the sensor system.

Index Terms—Sensing, energy harvesting, energy storage, battery heating, energy neutral embedded systems.

I. INTRODUCTION

DURING the last decades, embedded sensor systems (in particular wireless sensor networks) were usually battery-powered and the main design paradigm to prolong the system lifetime was energy consumption minimization. There are different techniques for reducing energy consumption of wireless sensor systems applicable on different system levels: for sensing (e.g., compressive sensing [1], context-aware sensing [2], event-driven sensing [3]), for processing (e.g., dynamic voltage scaling [4], energy-aware scheduling [5]), for communication (e.g., duty-cycling [6], low-power MAC protocols [7]), and for combination of them (e.g., sensing and communication [8]). With the advance of energy harvesting technologies, new trends are focused on optimal distribution of energy consumption to maximize lifetime beyond the energy storage limits, leading towards reducing the maintenance costs

Manuscript received December 21, 2016; revised March 27, 2017; accepted March 27, 2017. Date of publication April 6, 2017; date of current version May 5, 2017. The associate editor coordinating the review of this paper and approving it for publication was Dr. Wan-Young Chung. (*Corresponding author: Vana Jelcic.*)

D. Cesarini and M. Marinoni are with the Real-Time Systems Laboratory, Scuola Superiore Sant'Anna, 56124 Pisa, Italy (e-mail: daniel.cesarini@sssup.it; mauro.marinoni@sssup.it).

V. Jelcic, M. Kuri, and V. Bilas are with the Department of Electronic Systems and Information Processing, Faculty of Electrical Engineering and Computing, University of Zagreb, 10000 Zagreb, Croatia (e-mail: vana.jelcic@fer.hr; marijan.kuri@fer.hr; Vedran.Bilas@fer.hr).

D. Brunelli is with the Dipartimento di Ingegneria Industriale, University of Trento, 14 I-38123 Trento, Italy (e-mail: davide.brunelli@unitn.it).

Digital Object Identifier 10.1109/JSEN.2017.2691580

of such systems [9]. Although environmental energy can be unlimited, usually it is not constant in time and in space. Thus, it is necessary to design systems able to adapt their energy consumption to the scavenged energy, to achieve energy neutrality [10] — the ability of a system to operate in an uninterrupted way, with a self-sustained energy balance [11].

Alongside with the importance of harvesting, another key issue to develop energy-neutral systems is the ability to properly store and use energy to and from the storage element (such as a battery). Extreme temperature conditions usually reduce charge acceptance for battery chemistry, reducing allowed charging levels, and as a consequence can lead to the loss of precious energy. However, in a real-world environment, battery heating, especially using harvested energy which could not be stored, can represent a solution to partially cope with these problems, when the cost of heating is largely compensated by the extra-energy that the energy storage device can accumulate.

In this paper we focus on energy harvesting and on ensuring that energy could be stored in the batteries through battery heating. We present a general model of an energy harvesting sensor system and a particular implementation that we built and tested in outdoor environment. The significant elements and the internal signals of the system are monitored, allowing us to follow all phenomena related to solar harvesting and put them into relation with the environment (i.e., weather condition changes regarding clouds, fog, sun, temperature, etc.). Our case study shows that heating the battery in sunny and low-temperature (below 0°C) weather conditions allows storing otherwise lost energy. The example of a sunny and cold winter day demonstrates that a significant amount of energy can be saved for possible later exploitation, if a (small) amount of energy is diverted for heating directly from the solar panel. Our results show that we saved more than 20000 J during that day, which suffice to power the system for 55 h.

The contribution of this paper is twofold:

- We show the benefits of battery heating for energy-harvesting sensor systems with Li-ion batteries under cold and sunny conditions. To the best of authors' knowledge, this is the first paper that provides an analysis of battery heating for energy harvesting embedded sensor systems;
- We verify our assumptions in an experimental setup with a real-world energy harvesting embedded sensor system. As emphasized in [11], the literature on energy harvesting lacks from real-world experiments on harvesting systems,

that would validate numerous existing theories and models, and allow gaining a deeper understanding of optimal design. We, thus, consider that one of the important aspects of our work is providing a real-implemented and long-tested harvesting system coupled with techniques, such as battery heating, that has been in operation for three years outdoor, at the time of writing this manuscript.

The remainder of the paper is organized as follows. Related work is given in Section II. Section III presents a general model of an energy harvesting embedded sensor system. The architecture of our system is described in Section IV. The case study, experimental setup and results are described in Section V. Section VI discusses the results and the experience gathered in the development of the system. Finally, Section VII concludes the paper and provides some future directions.

II. RELATED WORK

More than a decade ago, research in the field of embedded systems started to inspect energy harvesting technologies. There are different energy harvesting techniques [12], e.g., solar, wind, or vibration harvesting. Furthermore, there are systems that combine different harvesting techniques to obtain more energy and a stable energy flow [13].

A. MPPT

To increase the efficiency of a harvester (i.e., extract the maximum power), many of them implement a Maximum Power Point Tracking (MPPT) circuitry. There are different MPPT techniques, depending on the system requirements [14]. We base our solar harvester on a MPPT technique presented by Lopez-Lapena *et al.* in [15], due to its simplicity, low power consumption and high efficiency. This MPPT device consists of an input capacitor constantly charged by the solar panel, the control circuitry, and the step up converter which periodically provides partial discharges of the input capacitor, transferring charges to the buffer. It keeps the panel voltage within a window around the operating voltage. The control circuit tracks the *maximum power point* by nulling the difference of the panel average power of two successive time intervals within the charging interval.

B. Storage

Another important element to exploit the environmental energy is storing the harvested energy whenever the system generates more energy than needed at a certain time [16]. Energy storage elements ensure stable energy to the system, disregarding fluctuations in the environmental energy sources. Capacitors and supercapacitors are often used as short-term storage elements, supporting unlimited number of charge-discharge cycles. Batteries, on the other hand, are generally used for long-term energy storage. They usually withstand a limited amount of charge-discharge cycles. To recharge them, specialized circuits are needed, depending on the battery's technology (e.g., Li-ion, Ni-MH, Lead-acid). We designed a system with lithium-ion (Li-ion) batteries as long-term energy storage due to their high efficiency, low self-discharging and

high energy density (weight to capacity ratio). On the other hand, the choice of Li-ion over, e.g. Lead-acid batteries has also a drawback: it is not allowed to recharge the battery when its temperature is below 0°C because it can cause lithium plating on the anode which degrades life cycle [17] and can lead to explosion risks [18].

To cope with this problem, *battery heating* can be used to increase their temperature and improve the charging conditions. Batteries can be heated directly using the harvested energy, or using energy already stored in the battery itself (self-heating) and thus performing maximum of task before depletion, as introduced by Ji and Wang [19] for increasing the efficiency of electric car batteries. On the other hand, Mohany *et al.* [20] investigated an optimal strategy to heat Li-ion batteries from sub-zero temperatures. However, our paper presents benefits of battery heating for solar harvesting systems in environmental monitoring applications in which the incoming energy is unpredictable. We especially focus on environments with low temperatures. In such applications, it is important for the system operation (i.e., phenomena monitoring) to have some energy stored in case of long periods of low solar irradiance. By now there has not been any similar study of battery heating.

C. Energy Harvesting Experiments

There are numerous energy harvesting sensor nodes in the literature [21]. However, most of the papers in this topic cover only theory and simulations. Few of the reported studies focus on *real-world multi-year experiments* with energy harvesting systems [11]. In [22], a simulator for vibration energy harvesting system was developed and experimentally verified on a microgenerator. A solar harvester for long-term environmental monitoring scenarios, presented in [23], endorsed with a dynamic power management for enabling energy-neutral operation by adapting system duty cycle is shown to have survived for more than two years in-field.

Our system was developed for powering wireless sensor nodes in a network for monitoring olive orchards in project MasliNet [24]. Our harvesting system was also used to verify the functionality of a simulator intended to study and test the feasibility of designs for automatic weather stations powered by wind or sun [25]. This paper presents experimental verification and interpretation of the battery heating on a real-world solar harvesting system during cold winter days.

III. GENERAL MODEL OF ENERGY HARVESTING SENSOR SYSTEM

A simplified model of an energy harvesting embedded sensor system is depicted in Fig. 1. The model consists of the following blocks:

- (a) Harvester: any device that can exploit physical/chemical phenomena (e.g., solar, wind, vibration, thermal) to produce electric energy. It can include some form of Maximum Power Point Tracking, and integrates a short-term energy buffer.
- (b) Storage element: any device/component able to store electric energy (e.g., battery, (super)capacitor, fuel cell).

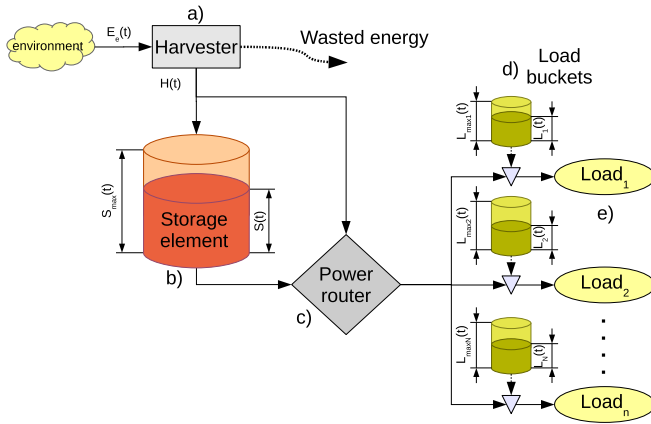


Fig. 1. Energy flow in an energy harvesting sensor system.

- (c) Power router: decides how to use/route the available energy in the system. It can be implemented using hardware or software solutions, and either as a single integrated component or as a set of different subsystems managing different functionalities.
- (d) Load buckets: represent the amount of work that needs to be performed by each load at a certain time. The size and occupation semantic varies depending on the type of load, e.g., a radio will have a *data-to-send* bucket, while a motor or other actuator will have an *activity-to-do* bucket.
- (e) Loads: implement functionalities to achieve the goals of the embedded system. Some examples are a microcontroller unit, a transceiver, a data storage device, and a set of sensors and actuators.

In particular, the harvester generates $H(t)$ in response to $E_e(t)$ (the environmental energy, which replenishes the storage element), characterized by $S_{max}(t)$ (maximal energy capacity, which can vary over time based on external conditions) and $S(t)$ that varies based on the amount of current that flows to the storage and the external conditions. The N loads are each related to a corresponding load service bucket/queue, with $L_{max}(t)$ and $L(t)$ as the maximum size of such a bucket and the actual bucket occupation, respectively. When considering a particular case of a system with battery heating we can change $S_{max}(t)$ by acting on the battery temperature. Moreover, we need to consider that $H(t)$ can only be used by the system loads and cannot be put into the battery if the Li-ion battery temperature is below a safety recharging threshold. Finally, we need also to consider that heating the battery not only can increase $S_{max}(t)$, but also $S(t)$ because the available capacity changes at a different battery temperature.

IV. SYSTEM CHARACTERISTICS

In this section we describe how our energy harvesting system has been implemented according to the model presented in Section III.

A. System Architecture

The block scheme of the implemented system is shown in Fig. 2. It is based on a solar panel, with a power of 5 W

(open-circuit voltage $V_{oc} = 21.6$ V; short-circuit current $I_{sc} = 0.32$ A). The energy collected by the solar panel is transferred by the MPPT circuitry to the Energy buffer for short-time storage, such as an electrolytic capacitor. The MPPT, built with analog components, is based on the concept presented in [15]. From the energy buffer the energy can be distributed to the loads, to the battery heater, or to the long-term storage such as a Li-ion battery.

The Storage control (a specialized charger) charges the batteries according to the information obtained from the Li-ion battery pack and the harvester. It is equipped with a thermostat, an additional device assigned to control the battery heater to keep the temperature of the Li-ion battery pack above the freezing point. The Power path control routes the energy to the loads by switching the loads between the available energy sources (Energy buffer and Li-ion battery pack).

The Energy buffer and the battery pack have different output voltages which are used by the Power path controller to determine their presence. Whenever there is energy in it, the energy is used from the Energy buffer, while the energy from the Li-ion battery pack can be used only when there is a lack of environmental (solar) energy. In the periods when the solar power is not enough to completely power all the loads, the Power path control is constantly switching and taking energy from both the Energy buffer and Li-ion battery pack. Load control block checks and manages the activity of each particular load.

One of the loads is a Wasp mote wireless sensor node [26]. It includes a microcontroller, a radio module and an interface board to adapt electrical signals of measured values (i.e., voltages, currents, irradiance, and panel temperature) to analog and digital inputs and to control two additional resistance loads (0.5 W and 1 W) with two digital outputs. These additional loads are used to simulate high-power devices, enabling larger static or dynamic variation of the system load.

The interconnection between the blocks is represented with switches (S_x) and multiplexers (M_x) which enable the control of the power flow in the system. The switches are the points at which the Power router can act to enable/disable energy flow, while the multiplexers are the units in charge for selecting which input to connect to a given output. The system contains the following switches and multiplexers:

- *Harvester switch* (S_H) enables/disables the energy flow from the harvester to the loads.
- *Harvester to Storage switch* (S_{HS}) enables/disables the recharge of the energy storage elements (Li-ion battery pack) with the energy coming from the harvester. It can be used to implement the load voltage conditioning.
- *Service multiplexer* (M_S) selects the power source for the service subsystem (in our case battery heating), either the harvester or the storage.
- *Load multiplexer* (M_L) selects the power source for the loads, either the harvester or the storage.
- *Load (i) switches* (S_{L_i}) enable/disable the powering of each single load of the system. Power is coming from M_L multiplexer.
- *Service switch* (S_S) enables/disables the powering of the service subsystem (battery heater). Power is coming

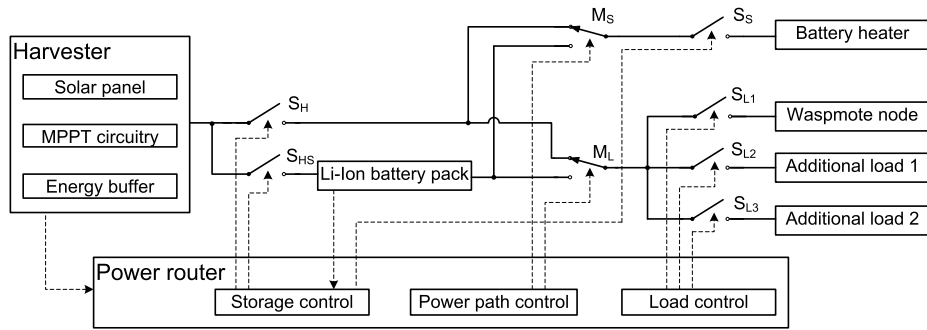


Fig. 2. Block scheme of the developed harvesting system.

from M_S multiplexer. It can be used to implement the load voltage conditioning.

B. Power Management

The designed harvesting system could be logically divided into power supply and loads. The power supply should collect, store and deliver the maximum of the available solar energy to the loads. The power supply is limited by the available solar energy over time, while the loads are limited by the ability of the power supply to collect and store available solar energy. The behavior of each subsystem should be adjusted to maximally exploit the available energy.

In the presented system, the *power supply power management* is a threshold selection strategy which drives units inside the power supply to operate in the right sequence. It provides stability to the power supply by balancing the harvester power from the energy buffer with the system consumption (loads, Li-ion battery pack heater and storage control), according to the set priorities. It is based on the Energy buffer voltage, used as the power balance indicator: if the input power to the buffer is higher than the output power, the buffer voltage is rising and *vice versa*. At the equilibrium, the buffer voltage is stable. According to varying conditions, control circuits balance the power. The priority of power consumption is set to the MPPT device: the first device to be powered when enough power is available is the MPPT. The MPPT is based on low-power components, and 10 W/m^2 of irradiance on the 5 W panel suffice to provide all the necessary power. Once there is enough power for the MPPT, the remaining power is used for the loads, while only the rest (if any) goes to the battery pack heater and/or to the battery charger. The balance between the input and the output power on the buffer is achieved by controlling the heater or the battery charging current. Note that in the case of discharged battery, the complete panel power can be used for charging and balance can be maintained even without the additional load. When the battery is almost full, the charging cannot continue (it reaches a constant voltage) and the exceeding energy will be wasted.

Load power management is the load control strategy performed by the wireless node (Load control). It controls the load activity. It can be sequential or dynamic (adaptive). For better presenting the effects of the adaptability of harvesting and storage management, in the present work we adopt a sequential load management. The sequential management

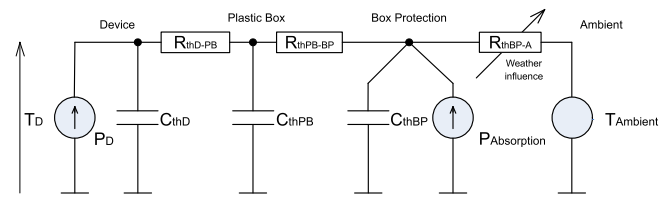


Fig. 3. An electric equivalent circuit of the thermal model of the harvesting electronics and batteries placed inside a plastic box coated with aluminum foil. P is the heat source, R is the thermal resistance and C the thermal capacitance. The device denotes electronic PCBs, heater and batteries fixed on an aluminum holder.

activates loads by the same sequence periodically, so the battery capacity should be large enough to cover a statistically-determined period without solar energy. It is exposed to both interrupts in operation and waste of available energy.

C. Battery Heating

At low temperature conditions, the solar panel efficiency is increased, but the storage (i.e., charging the Li-ion batteries) is not allowed, causing an increased amount of available energy which cannot be stored. Thus, it is worthwhile to exploit the options in which that energy surplus could be used to heat the batteries to a temperature acceptable for charging.

The battery heater in our system is designed to be powerful enough to dissipate all the power available from the panel. It is “U” shaped, closely surrounding the vertically placed battery pack positioned between two PCBs. The heating is convective, providing air flow by natural circulation. The heater is controlled by a thermostat and power management circuitry. The thermostat turns the heater on when the battery temperature decreases below 1.6°C and turns it off when the temperature rises above 3.8°C . The heating power depends on the difference between the available power from the panel and the power used by the loads.

Thermal model: To study the thermal behavior of the harvesting system, we developed an electric equivalent circuit of its thermal model. This model is shown in Fig. 3, and it comprises the *device* (the PCBs of the electronic system, the heater and the batteries fixed together on an aluminum holder) and the *plastic box* with an aluminum foil protection. The heating power (P_D) comes from the heater, the electronic circuits dissipation, and the battery self-heating, $P_{Absorption}$

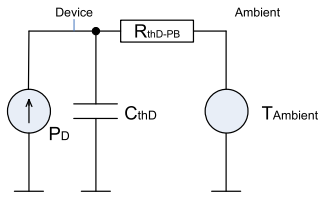


Fig. 4. A simplified electric equivalent circuit of the thermal model of the harvesting system. P is the heat source, R is the thermal resistance and C the thermal capacitance.

comes from the sunlight absorption, whilst the ambient conditions (temperature T_{Ambient} and wind) affect the thermal losses. The thermal capacitances are calculated from the specific thermal capacitance (J/gK) of each material and its mass (g) obtained by our measurements:

$$\begin{aligned} C_{\text{thD}} &= C_{\text{thBatt}} + C_{\text{thHeater}} + C_{\text{thHolder}} + C_{\text{thPCB}} \\ &= 1.00 \text{ J/gK} \cdot 46.6 \text{ g} \cdot 2 + 0.921 \text{ J/gK} \cdot 15.6 \text{ g} + \\ &\quad + 0.921 \text{ J/gK} \cdot 76.1 \text{ g} + 0.600 \text{ J/gK} \cdot 75.8 \text{ g} \\ &= 93 + 14.4 + 70.1 + 45.5 = 223 \text{ J/K}; \end{aligned} \quad (1)$$

$$C_{\text{thPB}} = 1.25 \text{ J/gK} \cdot 345 \text{ g} = 431 \text{ J/K}. \quad (2)$$

C_{thBP} is negligible due to a very low mass of the aluminum foil. The thermal resistance between the device and the box $R_{\text{thD-PB}} = 9.3 \text{ K/W}$ is calculated from the thermal time constant of the system (2070 s) that we measured, and the calculated thermal capacitance C_{thD} . We assumed that the large surface and the thin walls of the plastic box, as well as the thin aluminum foil around it and the measured wind speed in the range of 4 – 12 km/h make the thermal resistances $R_{\text{thBP-A}}$ and $R_{\text{thPB-BP}}$ negligible compared to $R_{\text{thD-PB}}$:

$$R_{\text{thPB-BP}} \ll R_{\text{thD-PB}} \quad (3)$$

$$R_{\text{thBP-A}} \ll R_{\text{thD-PB}}. \quad (4)$$

Furthermore, assuming that the sunlight contribution to the heating is much smaller than the heater's contribution, because the box is placed in the shadow of the panel, we propose a simplified thermal model (Fig. 4) that enables a quick estimation of the relations between the power provided to the heater (P) and the time needed to rise the temperature of the batteries (to the normal operating range) under specific ambient conditions. From this simplified model it is possible to obtain characterizing equations, omitted for the sake of simplicity, and to calculate a) the *time* needed to reach a given temperature with a given power, or b) the *power* needed to reach a given temperature with a given time. For illustration, should the batteries' temperature rise from -4°C , or 0°C , or 1.6°C to the working point of 3.8°C , the minimal required power to reach that temperature would be 0.83 W, 0.41 W or 0.24 W, respectively and the heating would last for 172.5 minutes (5 thermal time constants). Finally, consider that, as we show in Section V-B, power levels higher than minimal enable a faster battery temperature rise.

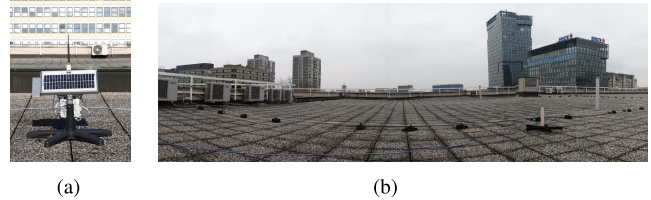


Fig. 5. The deployed harvesting system. (a) Harvester – front view. (b) The field of view from the roof of the building where the system is placed.

D. Energy Efficiency

System efficiency is a measure of the harvesting system behavior. It is described by the ratio of the energy provided to the loads and available solar energy. It represents the system ability to utilize the available power. It is related to the system and load power management which has to (i) constantly run the main tasks, (ii) store maximal energy for the future, and (iii) use the energy surplus to run additional tasks of lower importance. From a point of view of efficiency, a system with a sequential load management set to survive the winter period will be excessive for the summer time, when it will have large energy surpluses and low efficiency.

Harvester efficiency is a characteristic of the harvester circuitry. It is described by the ratio between the (average) harvester output power and the available panel power.

V. CASE STUDY

This section presents some experiments on the previously described system to show that:

- the battery heating and the appropriate battery management increases the overall availability of the system;
- the heating allows to exploit otherwise lost energy.

A. Experimental Setup

To carry out the experiments, the system described in Section IV has been placed on the roof of one of the University buildings in Zagreb. The front view of the system taken on the roof is depicted in Fig. 5(a). The panoramic view from the system to the sky is depicted in Fig. 5(b). The system has been working there for more than 3 years, almost continuously.

Three ambient parameters are measured: irradiation, panel temperature and system temperature. The irradiation sensor is placed on the top of the solar panel. The temperature sensor is attached to the back side of solar panel. The system temperature is measured inside the box using the Waspnote on-board temperature sensor.

The microcontroller on the Waspnote node monitors (all) the relevant currents and voltages of the system and stamps them with the related times. The information about the system state is acquired every 10 seconds, and the data is stored in the SD memory card. Every 30 minutes, the acquired data is read from the SD memory and transmitted over the radio link.

Furthermore, some measurements have been performed in laboratory in a controlled climate setting to obtain temperature dependence data for other measurements.

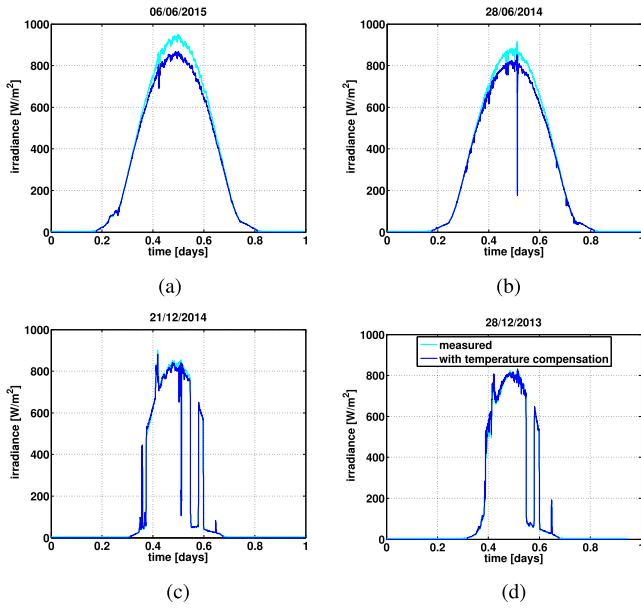


Fig. 6. Irradiance in summer time (a) and (b) and in winter time (c) and (d). The low irradiance in the morning and in the afternoon in winter time is due to fog and shadow caused by the skyscrapers on the horizon, while the peak before noon is the reflection from their glass surface (Fig. 5(b)).

B. Experimental Results

From the deployed system we obtained valuable insights about the actual irradiance level throughout the year. Moreover, thanks to measurement probes in the system electronics, we can provide evidence on how the power path control and the storage control act on the system, with particular emphasis on the battery heating system.

1) *Available Energy From the Panel*: Our measurements show changes in the amount of the maximum available energy during the year. Fig. 6 presents the irradiance measured on the solar panel of the system mounted at the rooftop of the University building in Zagreb, for clear days close to the summer and winter solstice, respectively. From the measured irradiance and the temperature dependence of the used panel, we calculate the available energy. These measurements show that the maximum available energy in the winter solstice is approximately 58% of the energy available in the summer solstice (i.e., 70 kJ vs. 120 kJ).

2) *Harvester Efficiency*: In the periods of low irradiance (10 W/m^2), the available panel power is barely sufficient to keep the MPPT circuit in the working condition. As there is no available power on the harvester output, the harvester efficiency is very low. As the panel power increases, the usable power increases with respect to MPPT circuit consumption and power conversion losses, causing the increment of the harvester efficiency, shown in Fig. 7.

3) *Battery Heating Phenomena*: Hereafter we present the system behavior for a winter day with the temperature lower than 0°C . In particular, we consider a day (27.1.2014), designated as D^{W0} in the remainder of this manuscript, that was windy with east wind which was changing speed from 4 to 12 km/h. The temperature varied from -6°C at 8 h in the morning to -1°C at 14 h and -3°C at 16 h.

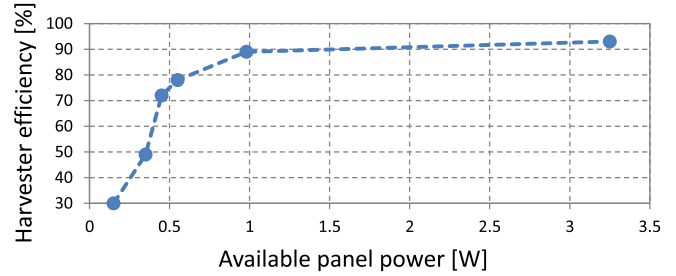


Fig. 7. The harvester efficiency at varying panel power levels.

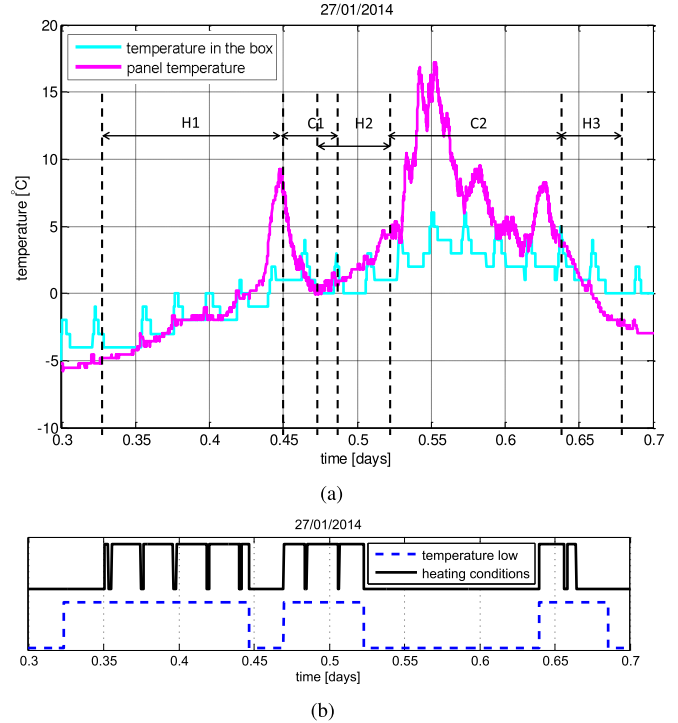


Fig. 8. Temperature in the box and temperature on the solar panel on the cold day D^{W0} (when ambient temperature did not rise over 0°C), with control signals for heating. (a) Temperature measurements on 27.1.2014, with characteristic heating and charging periods. (b) Control signals for heating: temperature low and heating conditions.

According to the harvester activity, the day D^{W0} can be divided in 5 periods with alternating freezing and non-freezing conditions, as presented in Table I and depicted in Fig. 8(a). Heating and charging periods are separated according to the low temperature status from the battery temperature protection device built in the charger. The overlapping of the first charging period (C1) and the second heating period (H2) is made to avoid a discontinuity in the low temperature signal or the heating period in the diagrams. In this overlapping period, the heating regularly started and reduced charging to the absolute minimum before the battery temperature fell to the critical level and the protection device disabled charging. More in particular:

- *H1 (heating)*: The first heating period (H1) starts in the morning at the harvester start-up. At that time, the panel temperature was -5°C , the inbox temperature -4°C ,

TABLE I
DISTRIBUTION OF HARVESTED ENERGY OVER DIFFERENT ACTIVITY PERIODS

Period	H1 (heating)	C1 (charging)	H2 (heating)	C2 (charging)	H3 (heating)	total
Time interval	7:56–10:43	10:43–11:35	11:16–12:32	12:32–15:21	15:20–16:26	7:56–16:26
Duration [s]	10021	3135	4613	10109	3960	30636
Theoretically available energy on/from panel E_A [J]	7020	3780	5590	22600	1250	39000
Energy delivered by buffer, E_B [J]	1120	3030	1130	19600	283	24600
Charging energy delivered by buffer, E_C [J] *	13	2640	493	18000	0	20600
Load energy delivered by buffer, E_D [J] *	941	340	557	1460	222	3440
MPPT device energy delivered by buffer, E_E [J] *	168	55	78	182	62	524
Heating energy delivered by buffer, E_F [J] **	4800	500	3960	20	719	9489

* — Energies calculated from the measured device consumption. Their total is presented in the row with energy delivered by buffer.

** — Calculated as a difference between theoretically available energy on buffer calculated from theoretically available energy on panel by means of measured harvester efficiency and measured energy delivered by buffer.

while the irradiance reached 18 W/m^2 that is 0.1 W of potentially available power from the panel. This power was exactly sufficient to start the harvester and supply energy to the MPPT circuitry. The increase of the irradiance level to 0.2 W of potentially available power from panel became sufficient to supply the basic Waspnote node operation of measuring and storing data. A further increment of irradiation started to produce a surplus of energy which was directed to the battery pack heater to heat the battery pack above freezing temperature.

During this period approximately 4800 J were used to heat up the battery pack temperature to 3.8°C , while at the same time the Waspnote node board inside the box went from -4 to 1°C . The fast rise of irradiation increased the heating power to approximately 2.5 W at 10:36:03 when the in-box temperature was 0°C . The system switched off the battery heating at 10:43:15, after 432 s . This time correlates with the results of our model presented in Fig. 4, that predicts that the heating from 0°C to 3.8°C lasts for 448 s under assumption that the heating power and the ambient temperature do not change significantly during that interval.

- *C1 (charging)*: Turning off the heater instantly enabled redirection of the energy surplus to the charging, so that in the charging period C1 the harvester provided 2640 J to the battery pack.
- *H2 (heating)*: The cold weather and the wind cooled the box again and the battery pack temperature hit the lower threshold again, thus the battery heating started again (H2). This period finished with the same conditions as the first heating period, spending 3960 J from the theoretically available 5590 J to heat the battery pack and devices inside the box.
- *C2 (charging)*: The second charging period (C2) was characterized by a rise of ambient air temperature up to -1°C which caused a reduced cooling of the box. This period charged the battery pack with 18000 J from the theoretically available 22600 J .
- *H3 (heating)*: In the last period H3, the irradiance level quickly reduced from 180 to 10 W/m^2 , leaving the MPPT device out of energy. The reduced ambient temperature of -3°C and the 719 J spent on heating did not create the charging conditions again.

Fig. 8(a) shows the temperature inside of the box and on the solar panel during the sunlight period of the day D^{W0} . One can notice that the temperature values in the box follow the trend of the panel temperature values. There is a difference and a noticeable delay in the average temperature values that can be explained by the presence of the insulation provided by the box and the fact that the panel is casting a shadow on the box. Moreover, the use of the on-board sensor has some drawbacks: it measures the Waspnote node board temperature, that is influenced by the node's activity, and every additional node activity increases power consumption, thus producing a corresponding rise of the board temperature. In the presented diagrams it can be seen as 3°C pulses caused by the data transmission interval occurring every half an hour.

The battery heating is evident during the period H1 (Fig. 8(a)) when the in-box temperature shows an increment of 5°C . The absence of battery heating is evident in the period C2 when the in-box temperature is almost stable although the panel temperature exhibits a high peak due to an abundance of available solar energy. In fact, battery heating raises in-box temperature by tracking the difference of available heating power and box thermal losses, restoring the charging conditions if possible.

The control signals for the battery pack heating are shown in Fig. 8(b). Please notice that the heating is enabled when the heating conditions are active (signal value '1') and the temperature is low (signal value '1'). These diagrams confirm the existence of three heating periods (H1, H2, H3) as shown in Fig. 8(a).

Fig. 9 shows the distribution of the energies spent in the system during during the observed day D^{W0} . The potentially available energy is the maximum that could have been harvested from the solar panel, as calculated from the irradiance, panel power and temperature. The load energy extracted from the buffer is spent for the node operation, resulting in a linear behavior. The charging energy extracted from the buffer is constant during low temperature periods and rises only during the charging periods C1 and C2. The energy used for supplying the MPPT device is low compared to the others and thus omitted. A significant part of energy is spent to heat the batteries, and thus called battery heating energy.

These energies enable the calculation of the (harvesting) system efficiency, shown in Fig. 10. The harvester efficiency

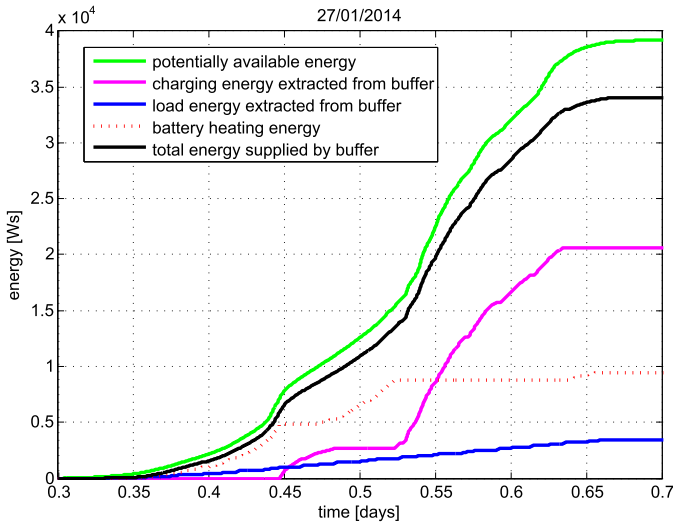


Fig. 9. Distribution of the energy spent in the system.

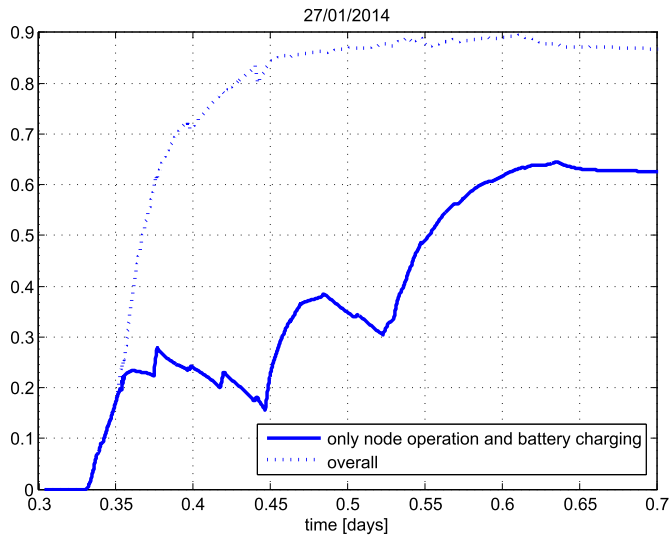


Fig. 10. Harvesting system efficiency with and without battery heating.

is calculated in two different ways: (i) considering the energy used only for node operation and charging battery; (ii) considering the overall harvester efficiency which includes all energies supplied by the buffer and used for node operation and the energy used for battery heating. In fact, the overall efficiency of the harvesting system reaches 90% when the battery heating is active. This confirms the connection between high-power loads (e.g., battery heating) and high efficiency of the system.

VI. DISCUSSION

In the proposed system, the use of battery heating allows to store more energy than the solution without heating. This capability, especially in cold but sunny days, increases the overall active time and availability of the system. In fact, the more energy it stores during the sunny cold weather, the more energy will be available from the battery during the possibly cloudy weather afterwards. The energy ΔE that

was stored allows the system to function for a Δt longer than without it.

The measurements from the cold and sunny day, D^{W0} , presented in the previous section show that the heating enables charging of $\Delta E_1 = 2640$ J in the first charging period (C1). That energy suffices for surviving $\Delta t_1 = 7$ h (each 0.5 h-period needs approximately 186 J for measuring, storing and transmitting data). The second charging period (C2) assures $\Delta E_2 = 18000$ J of stored energy — enough for $\Delta t_2 = 48$ h of continuous operation.

With the assumption that the system energy storage is completely empty at the beginning of the operations in the morning, the system starts to work when there is enough irradiance to power the MPPT and the system loads (i.e., around 8 h in the morning, as can be seen in Fig. 8(a)). Without the heating capability, during that day the low temperature would have prevented the battery recharging and thus the system would stop working when there would not be enough energy on the panel anymore (i.e., around 16:30 h in the afternoon).

However in our case, with the battery heating, the energy accumulated during that particular day D^{W0} equals to $\Delta E = \Delta E_1 + \Delta E_2 = 20640$ J, corresponding to $\Delta t = \Delta t_1 + \Delta t_2 = 55$ h. As the entire day D^{W0} was sunny, the system used the energy directly from the solar panel, without using the energy accumulated in the battery. In other words, the Δt transfers directly into increment of active time of the system. Thus, the system would be able to survive the night and 2 whole days afterwards, even if there would not be enough energy from the solar panel. That increases the active time of the system in worst-case scenario (i.e., without enough irradiance) and increases the reliability of the system (i.e., the probability of detecting and reporting an interesting event). With this we demonstrate the proof of concept that the battery heating permits to store and use otherwise lost energy. Finally, this enables a longer system lifetime in the direction of perpetual operation.

Following the example provided by [19] for battery heating in electric cars, it would also be possible to exploit the energy stored inside the batteries to heat them and gain some more capacity. However, as opposed to the goal of a car to cover a certain distance in a short time, the goal of a monitoring system is to stay alive for a long time. In the case of alarm systems, battery heating using the internal energy could be beneficial when the energy spent increases the short-term capacity of the buffers, thus allowing to transmit an important message.

VII. CONCLUSION

Energy harvesting sensor systems are key components of isolated environmental monitoring systems, performance of which is directly correlated to available energy for operation. In this paper we introduce a general model of an energy harvesting sensor system and present a specific methodology for design and evaluation of such systems applied in environmental monitoring. We present a case study on improving the availability of the system by smart usage of the harvested

energy to extend operating temperature range of the long-term storage unit (Li-ion). We show that during a cold sunny winter day we are able to store otherwise lost energy by heating the battery above the freezing point and thus enabling energy storage. In particular, our results show that the battery heating ensured storing enough energy for 55 h of system operation, which is more than a double compared to the case when battery heating is not used. Our future work will focus on adaptive energy management techniques (both on the energy consumption and on the energy harvesting side), leading towards designing an energy-neutral system.

REFERENCES

- [1] Y. C. Eldar and G. Kutyniok, *Compressed Sensing: Theory and Applications*. Cambridge, U.K.: Cambridge Univ. Press, 2012.
- [2] V. Jelacic, M. Magno, D. Brunelli, G. Paci, and L. Benini, "Context-adaptive multimodal wireless sensor network for energy-efficient gas monitoring," *IEEE Sensors J.*, vol. 13, no. 1, pp. 328–338, Jan. 2013.
- [3] L. Liang, D. Gao, H. Zhang, and O. W. W. Yang, "Efficient event detecting protocol in event-driven wireless sensor networks," *IEEE Sensors J.*, vol. 12, no. 6, pp. 2328–2337, Jun. 2012.
- [4] M. Bambagini, F. Prosperi, M. Marinoni, and G. Buttazzo, "Energy management for tiny real-time kernels," in *Proc. Int. Conf. Energy Aware Comput. (ICEAC)*, Nov. 2011, pp. 1–6.
- [5] L. Santinelli, M. Marinoni, F. Prosperi, F. Esposito, G. Franchino, and G. Buttazzo, "Energy-aware packet and task co-scheduling for embedded systems," in *Proc. 10th ACM Int. Conf. Embedded Softw.*, 2010, pp. 279–288.
- [6] R. C. Carrano, D. Passos, L. C. S. Magalhaes, and C. V. N. Albuquerque, "Survey and taxonomy of duty cycling mechanisms in wireless sensor networks," *IEEE Commun. Surveys Tuts.*, vol. 16, no. 1, pp. 181–194, 1st Quart., 2013.
- [7] P. Huang, L. Xiao, S. Soltani, M. Mutka, and N. Xi, "The evolution of MAC protocols in wireless sensor networks: A survey," *IEEE Commun. Surveys Tuts.*, vol. 15, no. 1, pp. 101–120, 1st Quart., 2013.
- [8] V. Jelacic, M. Magno, D. Brunelli, V. Bilas, and L. Benini, "Benefits of wake-up radio in energy-efficient multimodal surveillance wireless sensor network," *IEEE Sensors J.*, vol. 14, no. 9, pp. 3210–3220, Sep. 2014.
- [9] C. Moser, L. Thiele, D. Brunelli, and L. Benini, "Adaptive power management for environmentally powered systems," *IEEE Trans. Comput.*, vol. 59, no. 4, pp. 478–491, Apr. 2010.
- [10] A. Kansal, J. Hsu, S. Zahedi, and M. B. Srivastava, "Power management in energy harvesting sensor networks," *ACM Trans. Embed. Comput. Syst.*, vol. 6, no. 4, p. 32, Sep. 2007. [Online]. Available: <http://doi.acm.org/10.1145/1274858.1274870>
- [11] D. Gunduz, K. Stamatiou, N. Michelusi, and M. Zorzi, "Designing intelligent energy harvesting communication systems," *IEEE Commun. Mag.*, vol. 52, no. 1, pp. 210–216, Jan. 2014.
- [12] A. S. Weddell, M. Magno, G. V. Merrett, D. Brunelli, B. M. Al-Hashimi, and L. Benini, "A survey of multi-source energy harvesting systems," in *Proc. Conf. Design, Autom. Test Eur. Conf. Exhibit. (DATE)*, 2013, pp. 905–908.
- [13] M. Magno, D. Boyle, D. Brunelli, B. O'Flynn, E. Popovici, and L. Benini, "Extended wireless monitoring through intelligent hybrid energy supply," *IEEE Trans. Ind. Electron.*, vol. 61, no. 4, pp. 1871–1881, Apr. 2014.
- [14] T. ESRAM and P. L. Chapman, "Comparison of photovoltaic array maximum power point tracking techniques," *IEEE Trans. Energy Convers.*, vol. 22, no. 2, pp. 439–449, Jun. 2007.
- [15] O. López-Lapeña, M. T. Penella, and M. Gasulla, "A new MPPT method for low-power solar energy harvesting," *IEEE Trans. Ind. Electron.*, vol. 57, no. 9, pp. 3129–3138, Sep. 2010.
- [16] J. Cho, S. Jeong, and Y. Kim, "Commercial and research battery technologies for electrical energy storage applications," *Progr. Energy Combustion Sci.*, vol. 48, pp. 84–101, Jun. 2015.
- [17] A. Paryani, "Low temperature charging of Li-ion cells," U.S. Patent 0012562 A1, Jan. 20, 2011. [Online]. Available: <http://www.google.com/patents/US20110012562>
- [18] J.-M. Tarascon and M. Armand, "Issues and challenges facing rechargeable lithium batteries," *Nature*, vol. 414, no. 6861, pp. 359–367, 2001.
- [19] Y. Ji and C. Y. Wang, "Heating strategies for Li-ion batteries operated from subzero temperatures," *Electrochimica Acta*, vol. 107, pp. 664–674, Sep. 2013.
- [20] S. Mohany, Y. Kim, A. G. Stefanopoulou, and Y. Ding, "On the warmup of Li-ion cells from sub-zero temperatures," in *Proc. Amer. Control Conf. (ACC)*, Jun. 2014, pp. 1547–1552.
- [21] S. Sudevalayam and P. Kulkarni, "Energy harvesting sensor nodes: Survey and implications," *IEEE Commun. Surveys Tuts.*, vol. 13, no. 3, pp. 443–461, 3rd Quart., 2011.
- [22] T. J. Kazmierski, L. Wang, B. M. Al-Hashimi, and G. V. Merrett, "An explicit linearized state-space technique for accelerated simulation of electromagnetic vibration energy harvesters," *IEEE Trans. Comput.-Aided Des. Integr. Circuits Syst.*, vol. 31, no. 4, pp. 522–531, Apr. 2012.
- [23] B. Buchli, F. Sutton, J. Beutel, and L. Thiele, "Dynamic power management for long-term energy neutral operation of solar energy harvesting systems," in *Proc. 12th ACM Conf. Embedded Netw. Sensor Syst.*, 2014, pp. 31–45.
- [24] V. Jeličić, T. Ražov, D. Oletić, M. Kuri, and V. Bilas, "MasliNET: A wireless sensor network based environmental monitoring system," in *Proc. 34th Int. Conv. (MIPRO)*, May 2011, pp. 150–155.
- [25] D. Cesarini, L. Cassano, M. Kuri, V. Bilas, and M. Avvenuti, "AENEAS: An energy-aware simulator of automatic weather stations," *IEEE Sensors J.*, vol. 14, no. 11, pp. 3932–3943, Nov. 2014.
- [26] Libelium Comunicaciones Distribuidas S. L. (2012). *Waspnote datasheet*. [Online]. Available: <http://www.libelium.com/v11-files/documentation/waspnote/waspnote-datasheeteng.pdf>



Daniel Cesarini received the B.Sc., M.Sc., and Ph.D. degrees in computer engineering from the University of Pisa, Italy, in 2006, 2010, and 2014, respectively. During the Ph.D., he focused on wireless sensor networks applied to human-motion tracking for real-time acoustic feedback (sports related) and on solar powered wireless systems for harsh environments. He has two years of Post-Doctoral Research experience with the Scuola Superiore Sant'Anna, under the Supervision of Prof. G. Buttazzo and Dr. M. Marinoni, where he was involved

in a wireless sensor system for human motor tele-rehabilitation. His main research interests are networked embedded systems, human-computer interaction, and energy harvesting systems.



Vana Jelacic (S'09) received the Ph.D. and M.S. degrees in electrical engineering from the Faculty of Electrical Engineering and Computing, University of Zagreb, Zagreb, Croatia, in 2014 and 2009, respectively. She was a Visiting Researcher with the Department of Electrical Engineering and Computer Science, University of Bologna, Bologna, Italy, from 2010 to 2012. In 2015, she was a Post-Doctoral Researcher with the Faculty of Electrical Engineering and Computing, University of Zagreb. Her main research interests include smart sensors and wireless sensor networks (WSNs), with focus on power management in WSNs with high-consuming sensors.



Marijan Kuri received the B.Sc. and M.Sc. degrees in electrical engineering from the University of Zagreb, Zagreb, Croatia, in 1989 and 1994, respectively. He was a Senior Analog Designer at Xylon, Zagreb. Since 2001, he has been a Technical Associate with the Department of Electronic Systems and Information Processing, Faculty of Electrical Engineering and Computing, University of Zagreb. His current interests include energy harvesting, low-power converters, and storage elements.



Mauro Marinoni received the M.Sc. and Ph.D. degrees in computer engineering from the University of Pavia, Italy, in 2003 and 2007, respectively. Since 2007, he has been with the Institute of Communication, Information and Perception Technologies, where he is currently an Area Leader of Resource Management with the Real-Time Systems Laboratory (ReTiS). He is an Assistant Professor with the Scuola Superiore Sant'Anna, Pisa. His leading research topics cover scheduling theory, operating systems and energy management for real-time systems,

focusing on the integration of real-time enhancements in different application fields, from e-Health devices to autonomous systems and distributed systems. He has been Local Coordinator of the FP7 JUNIPER Project and several industrial projects exploiting the ReTiS Lab research outcomes.



Davide Brunelli (M'10–SM'16) received the M.S. (*cum laude*) and Ph.D. degrees in electrical engineering from the University of Bologna, Bologna, Italy, in 2002 and 2007, respectively. He was a Visiting Researcher with ETH, Zurich, Switzerland, where he worked on methodologies for energy harvesting-aware embedded design. He was a Scientific Supervisor of several EU FP7 and H2020 projects, and was leading industrial cooperation activities with Telecom Italia, Italy, and STMicroelectronics. He is currently tenure track Associate Professor with

the University of Trento, Trento, Italy. His current research interests include smart grids and the development of new techniques of energy scavenging for Internet of Things (IoT) and embedded systems, the optimization of low-power and low-cost consumer electronics, and the interaction and design issues in embedded personal and wearable devices. He is leading the activity on energy efficiency in the IEEE Smart City initiative for the city of Trento. He is a member of several Technical Program Committees of conferences in the field of IoT and energy management.



Vedran Bilas (SM'10) is currently a Professor with the Faculty of Electrical Engineering and Computing, University of Zagreb, and the Head of the Laboratory for Intelligent Sensor Systems. He has over 20 years of research, development and technology transfer experience in the area of sensors and electronic systems. His research interests are in the field of energy efficient intelligent and networked sensors in various application domains.